

First Principles Study of Polyatomic Clusters of AlN, GaN, and InN. 2. Chemical Bonding

Aurora Costales,^{†,‡} Anil K. Kandalam,[§] A. Martín Pendás,^{†,⊥} M. A. Blanco,^{*,†,‡}
J. M. Recio,[†] and Ravindra Pandey[§]

Departamento de Química Física y Analítica, Universidad de Oviedo. 33006 Oviedo, Spain, and
Department of Physics, Michigan Technological University, Houghton, Michigan 49931

Received: December 7, 1999; In Final Form: February 17, 2000

In this paper we study the chemical bonding of the small (monomer, triatomic, and dimer) neutral clusters of AlN, GaN, and InN presented earlier in paper 1. It includes the analysis of the topology of the electron density and its Laplacian, together with relevant atomic properties, in light of the theory of atoms in molecules. The most prominent feature of the bonding here, the existence of strong N–N bonds, is seen to diminish with an increase in the number of metal atoms and the degree of ionicity. The Al–N bond shows a large transfer of charge, but also a significant deformation of the Al electron shells, so it can be understood as a highly polar shared interaction. On the other hand, Ga–N and In–N bonds are nonshared interactions, with smaller charge transfers and polarizations. In all cases, the existence of a N–N bond weakens the metal–nitrogen bond. The bonding picture that emerges depends only on the reliability of the electron densities, and it is consistent with the conclusions of our previous work in paper 1.

I. Introduction

The nitrides of aluminum, gallium, and indium and their alloys have received much recent technological effort, as stated in the previous paper,¹ referred to as paper 1 in the following. In this paper, we have reported a first principles investigation of the geometry, electronic structure, stability, and vibrational properties of small clusters of AlN, GaN, and InN within the generalized gradient approximation (GGA) to the density functional theory (DFT).

A clear picture of the complexity and richness of the chemical bonding in these systems emerges from the geometrical arrangements found. The most stable configurations are extremely dependent upon the relative stoichiometry of nitrogen atoms to metallic ones (*M*) and reflect the enormous dissimilarity of bonding mechanisms for the MN, MM, and NN pairs. Bonding patterns in these clusters are then very different from those found in the bulk. As nanoclusters become important in the manufacturing process of the solid nitrides,² it is expected that we need not only a thorough knowledge of the chemical bonding in the bulk, but also in molecules and small clusters. Furthermore, the evolution of the chemical bonding in nitrides when the metal atom is varied provides another interesting point for such an investigation.

A consistent, physically sound study of the chemical bonding in these polyatomics requires that extreme caution should be taken when using traditional orbital descriptions restated in the language of Kohn–Sham (KS) orbitals within the DFT. We have chosen, accordingly, the theory of atoms in molecules (AIM) of Bader³ to overcome these difficulties and arbitrariness. This is a fully quantum mechanical description of open subsystems that accounts for the physical properties of atoms

within molecules and their interactions. It focuses on the electron density as the primary observable. This means that its conclusions are independent of the method chosen to obtain the density. It also allows us to directly compare chemical bonding pictures coming from traditional wave function methods and those coming from DFT ones.

The rest of the paper is organized as follows. In section II, we briefly review the computational model used to obtain the electron densities and describe how the densities are fed into the AIM theory. Section III will present both the densities and their topological properties in the systems under study. We will finally comment on the bonding image emerging from our analysis, in section IV, and summarize our conclusions.

II. Methodology

The electronic structure and optimal geometries of all clusters studied here, MN, M₂N, MN₂, M₂N₂, and M₂N₂ in linear configurations, where M stands for Al, Ga, and In, was obtained in the generalized gradient approximation to the KS-DFT theory. Double numeric basis sets with d polarization functions (DNP), as implemented in the DMol code,⁴ were used. Details are fully discussed in paper 1 (previous paper in this issue). The current version of the AIM codes, as provided by Bader et al. in the AIMPAC suite of programs,⁵ does only allow for the density to be constructed as an orbital Gaussian expansion. To overcome these difficulties, we used the optimized DMol geometries reported in paper 1 to perform a single-point DFT Gaussian98⁶ calculation with the Becke⁷ exchange and Perdew–Wang⁸ correlation functionals used in the DMol optimizations. We have used the 6-31G** basis sets for N, Al, and Ga, and a double- ζ valence plus polarization (DZVP) basis set optimized for the DFT orbitals for In.⁹ The final densities obtained with this procedure were shown to be very similar to those in the DMol calculations by means of a careful comparison. Atomic properties have been obtained by integrating the appropriate observable densities over atomic basins. The precision of those integrations is always a matter of concern in topological analyses. In all the

* Corresponding author: Fax: (906) 487-2933. E-mail: mblanco@mtu.edu.

[†] Universidad de Oviedo.

[‡] Present address: Department of Physics, Michigan Technological University, Houghton, MI, 49931.

[§] Michigan Technological University.

[⊥] Present address: McMaster University, Hamilton, Ontario, Canada.

TABLE 1: Predicted Equilibrium Distances (bohr) for the Clusters under Study and Their Relevant Diatomic Pairs, As Obtained from the Calculations in Paper 1

system	R	system	R_{M-N}	R_{N-N}	R_{M-M}
$N_2, D_{\infty h}$	2.12				
$Al_2, D_{\infty h}$	4.72	AlN_2, C_s	4.07	2.18	
$Ga_2, D_{\infty h}$	5.28	GaN_2, C_s	4.71	2.15	
$In_2, D_{\infty h}$	5.99	InN_2, C_s	5.42	2.14	
$AlN, C_{\infty v}$	3.43	Al_2N_2, D_{2h}	3.97	2.45	7.55
$GaN, C_{\infty v}$	3.90	Ga_2N_2, D_{2h}	4.16	2.41	7.96
$InN, C_{\infty v}$	4.31	In_2N_2, D_{2h}	4.60	2.37	8.90
Al_2N, C_{2v}	3.31	$Al_2N_2, C_{\infty v}$	3.80	2.19	5.02
Ga_2N, C_{2v}	3.38	$Ga_2N_2, C_{\infty v}$	8.45	2.12	5.30
In_2N, C_{2v}	3.81	$In_2N_2, C_{\infty v}$	8.82	2.12	6.02

cases studied, the final value of the integral of the Laplacian of the density over every basin is smaller than 10^{-4} au.

In order to rationalize our AIM results, we have also obtained the electron densities of the M_2 , MN, and N_2 diatomic molecules using the Gaussian98 code and the same basis sets and functionals as described above. Calculations were made for a grid of internuclear distances covering the full range of interatomic separations found in the target clusters. This has allowed us to compare the bonding properties of the clusters to those of well-defined limiting molecules.

III. Results

In Table 1, we briefly summarize the optimal geometric parameters of the nitride clusters from paper 1 along with those of the homonuclear diatomics N_2 , Al_2 , Ga_2 , and In_2 . The agreement with the available experimental data is reasonable within the limits expected for the chosen model, as was shown in paper 1. One immediate conclusion is clear just from these data. The number of N atoms is controlling the type of basic metal–non-metal interaction. When there is just one N atom, the metal–non-metal interaction is a strong one. Whenever two nitrogen atoms exist, they do form a nitrogen molecule which, in turn, interacts weakly with the available extra metal atoms. What is even more interesting is that when the M_2N_2 clusters are considered, the linear isomers seem to be just a dinitrogen molecule interacting weakly with a dimetal molecule. However, the most stable configurations for AlN and GaN dimers are rhombic, and the rhombus structure is always a minimum of the energy surface. It is in the linear case where the different behavior of Al, Ga, and In is more clear.

We will first present the chemical bonding picture in the homonuclear diatomic molecules. We will then describe the first group of clusters, where the metal–nitrogen bond is dominant, and finally we will discuss our results when the dinitrogen bond is present.

A. Chemical Bonding in N_2 , Al_2 , Ga_2 , and In_2 . Table 2 is a summary of the relevant critical points of the electron density and their properties for the N_2 , Al_2 , Ga_2 , and In_2 systems. As expected, all of these molecules present just a symmetry fixed bond critical point along the internuclear axis. No nonnuclear attractors are found, even for aluminum. Differences in chemical bonding and in the atomic shell structure within the molecule are easily manifested by studying the Laplacian of the density. Figure 1 shows this scalar field for these molecules at the predicted optimum geometries in a plane containing the nuclei. The symmetry of the Laplacian is different for N_2 and Al_2 , on the one hand, and Ga_2 and In_2 , on the other hand. This is due to the different states of these molecules, of Σ_g symmetry for the nitrogen (spin singlet) and aluminum (spin triplet) dimers and of Π_u symmetry for the other two (both of them spin triplets).

TABLE 2: Topological and Atomic Properties for the N_2 , Al_2 , Ga_2 , and In_2 Molecules^a

	ρ	$\nabla^2\rho$	\mathcal{Q}	μ	\mathcal{Q}_b
N_2	0.638	-2.023	3.11×10^{-4}	0.591	1.359
Al_2	0.038	-0.019	1.62×10^{-4}	0.064	5.686
Ga_2	0.037	0.008	-3.08×10^{-6}	0.309	0.307
In_2	0.027	0.022	1.02×10^{-3}	0.276	0.042

^a This table contains the electron density (ρ), the Laplacian of the electron density ($\nabla^2\rho$) at the bond critical point, and also the atomic charge (\mathcal{Q}), the atomic dipole moment (μ), and the component of the traceless atomic quadrupolar moment tensor (\mathcal{Q}_b) along the internuclear axis. A positive dipole moment points toward the internuclear region, indicating an electron density concentrated in the opposite direction. A positive quadrupolar moment implies an oblate electron distribution. In homodiatomics, the absolute value of the atomic charge is a measure of the accuracy of the numerical integrations. All values in atomic units.

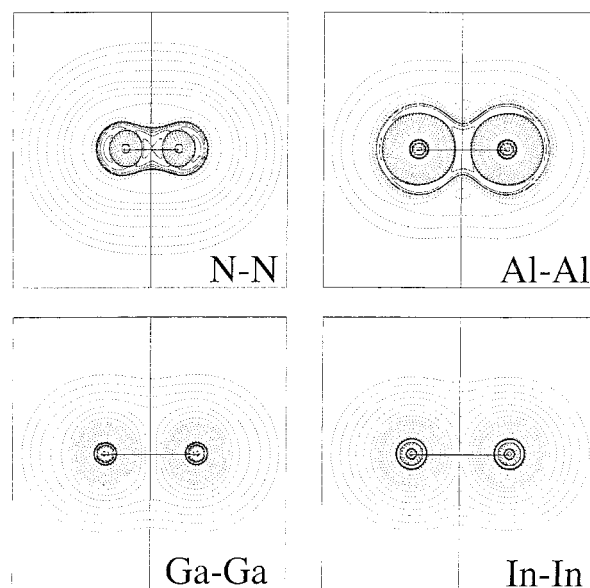


Figure 1. Laplacians of the electron density for the N_2 , Al_2 , Ga_2 , and In_2 homodiatomics in their fundamental states. All geometries are the predicted ones and are given in Table 1. The plotting plane is simply one containing the nuclei. Solid contours stand for negative values, while dashed ones, for positive ones. Both the interatomic surface projection and the bond path are also plotted. The intersection between them marks the position of the bond critical point.

We take for example the well-known behavior of N_2 . The valence shells of both nitrogens have fused together, the bond point is a (+3,+1) critical point (see ref 3) of the Laplacian, and it lies in the middle of a large negative region. There are two nonbonded charge concentrations behind the nitrogens along the nuclear axis and two bonded ones between them. This is the paradigm of a shared or covalent interaction. The atomic dipole of each nitrogen shows that the atomic density, as a whole, is displaced to the back side of the internuclear axis. The bond direction component of the traceless quadrupole tensor presents an oblate electronic ellipsoid consistent with the latter fact.

The Laplacian of Al_2 shows broken but fused valence shells with a single bonded charge concentration at the midpoint on the internuclear line and two large rings of degenerate (+2,+2) critical points encircling both atoms. The density and Laplacian at the bond point are roughly 15 and 100 times smaller than those in N_2 , respectively. The atomic dipole shows a much more spherical density, and the quadrupole is not to be misinterpreted. Its value is much greater than that in N_2 due to the larger

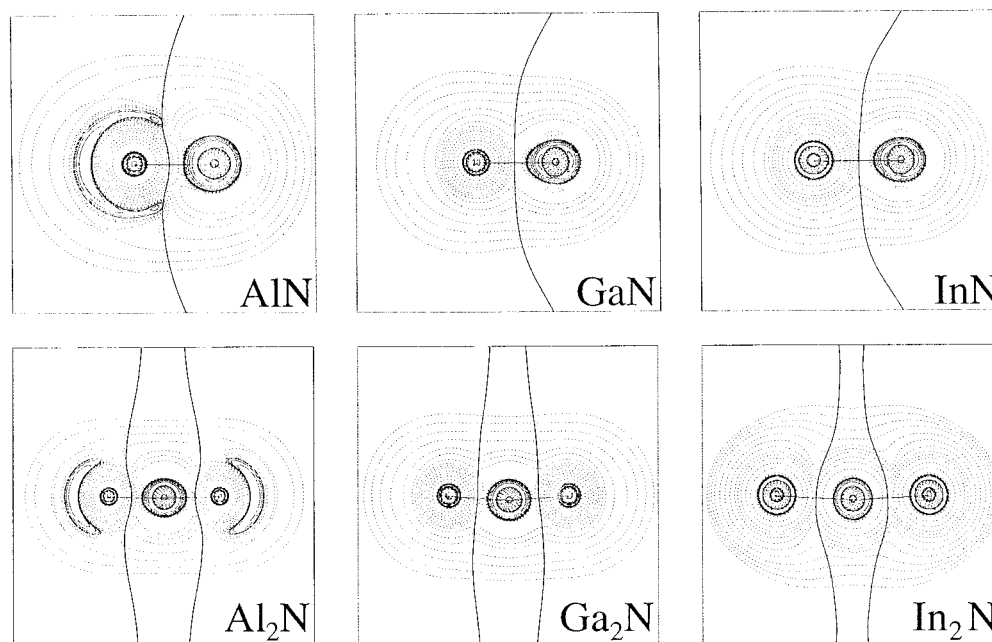


Figure 2. Laplacians of the electron density for the MN and M_2N clusters in a plane containing all nuclei at predicted equilibrium geometries. All symbols and labeling are the same as in Figure 1.

extension of the density. The interaction is shared, and there is a clear tendency toward the formation of a nonnuclear attractor in the internuclear region.

Ga_2 and In_2 , to the contrary, do not share external shells. Actually, their valence shells are not resolved from the next inner shells in the Laplacian, indicating that there is not a differentiated region of electron localization for the valence electrons. The small density and Laplacian values at the bond critical points are characteristic of nonshared interactions. It is interesting to notice that the bond direction component of the quadrupole decreases from Al_2 to In_2 , the latter displaying an almost spherical electronic distribution.

Also relevant to our discussion is how all of this picture evolves with interatomic distance. We have previously shown^{10,11} that as atoms approach and interact, the behavior of the electron density closely follows that of the overlap of atomic shells, giving rise to several regimes of interaction. As far as only distances involving the overlapping of the exterior (valence) shells are of interest, both the density and the Laplacian at bond points behave exponentially with distance. This general result applies to our case and will be very useful, as discussed below.

B. Chemical Bond in MN and M_2N clusters. Simple models of the chemical bonding in these molecules tend to focus on the large electronegativity difference between the metal and nitrogen atoms, leading to an usually very polar, covalent description of them. However, the picture emerging from our data does partially support that view only for the case of the aluminum molecules, and not for gallium and indium molecules.

Tables 3 and 4 show a collection of topological and atomic properties obtained from the optimal densities of paper 1 as described in section 2. Figure 2 shows the Laplacians in a plane containing the nuclei. AlN is a $^3\Pi$ molecule. The Al atom has given almost a full electron to the nitrogen atom. As a result of the net charge transfer, its valence shell is polarized strongly against the nitrogen. The valence electron density of the latter responds, polarizing itself toward the aluminum. As a result, both atoms display a rather large atomic dipolar moment. However, this deformation is also accompanied by an elongation of the density along the orthogonal direction, resulting in both

TABLE 3: Density (ρ) and Laplacian of the Density ($\nabla^2\rho$) at Bond Critical Points for the MN and M_2N Clusters^a

	r	ρ	$\nabla^2\rho$
AlN	0.58	0.081	0.526
GaN	0.53	0.086	0.238
InN	0.50	0.070	0.197
Al_2N	0.58	0.094	0.698
Ga_2N	0.51	0.126	0.614
In_2N	0.48	0.130	0.516

^a An asymmetry index $r = d_N/d$, where d_N is the distance from the bond point to the nitrogen atom and d is the total bond distance, is also shown. All data in atomic units.

TABLE 4: Atomic Properties for MN and M_2N Clusters^a

	atom	Q	μ	Q_b
AlN	Al	0.919	1.527	1.789
	N	-0.918	-0.732	1.025
GaN	Ga	0.542	1.375	0.219
	N	-0.542	-0.144	-0.594
InN	In	0.528	1.365	-0.013
	N	-0.528	-0.082	-0.452
Al_2N	Al	0.994	1.772	0.839
	N	-1.989	0.000	3.061
Ga_2N	Ga	0.691	1.314	1.825
	N	-1.382	0.000	5.046
In_2N	In	0.638	1.304	2.335
	N	-1.274	0.000	5.387

^a The table lists atomic charges, atomic dipole moments, and atomic quadrupole moment eigenvalues along directions approximately parallel to bonds. All data in atomic units and all symbols and conventions as in Table 2.

atomic densities being prolate with respect to the internuclear axis. In the case of aluminum, this behavior seems to show a still rather important interaction between its valence electrons and those of nitrogen. The value of the density at the bond critical point is rather low, as expected from the equilibrium distance, and the Laplacian is positive but relatively large. This picture corresponds to a polar dominated interaction with a rather low accumulation of density in the internuclear region coming from the polarization of the negatively charged nitrogen. The behavior of the interatomic surface in the proximity of the bond

point shows a convex aluminum and a concave nitrogen. This is rather typical, with cations having convex surfaces near bond points.¹² Another important point refers to spin densities. The integration of the spin density over the basin of the atoms shows 0.43 out of the 2.00 extra α electrons on the Al atom and the rest on the nitrogen. This effect will be more pronounced in the GaN and InN molecules.

No substantial changes to the bonding are observed for Al₂N. The molecule is quasilinear, and the charge transfer to the nitrogen is even larger than twice that found in the diatomic species, showing how aluminum is comfortable in its Al⁺ state and how nitrogen easily accepts two electrons. The atomic properties show that each aluminum is mostly the same object as in the diatomic if the variation in the bond distance is taken into account. If densities and Laplacians for the AlN molecule as a function of Al–N distance are used to predict the densities and Laplacians in Al₂N, we obtain 0.094 and 0.685 au, respectively. This kind of behavior, previously proven in other systems,¹¹ has also been found generally in the clusters under study.

GaN and InN, on the contrary, show a much smaller charge transfer which is unable to break the external electronic shell of the metals. The electronic polarizations, as coming from the atomic dipolar moments, show the same pattern as that in AlN, but now the effect is less important since the constancy of the metallic dipole against the increase in atomic size shows. Moreover, the N atom has now a prolate charge distribution, characteristic of a small interaction between the external electron shells of both atoms. The metallic atoms display very small quadrupole moments, showing the sphericity of its density, and the In atom is even slightly prolate. Densities and Laplacians are rather small, with values approaching those typical of simple closed-shell interactions.³ The interatomic surfaces are extremely planar near the bond critical point, a fact reflecting a very small electronic deformation. The main interaction is electrostatic in origin. This helps us to understand why there is such a strong shrinking in bond distances when a second metal atom is added. Both molecules have ³Σ states. The spin accumulation is now significant. Just 0.082 and 0.054 extra α electrons sit on the metal, respectively. This fact, together with the small charge transfer, implies a very simple model of electron pairing between the metal 2p unpaired electron and one of the three unpaired ones in the nitrogen quartet, leaving two lone unpaired electrons on the nitrogen. Much more could be said about electron pairing and localization if we had access to a well-behaved electronic pair density.

Ga₂N and In₂N are also quasi-linear molecules, like Al₂N, with significantly greater charge transfers than the monomers. Atomic dipole moments for the Ga and In atoms show that they are systems rather similar to those found in the diatomic species, but the increased negative charge in the nitrogen pushes them nearer, deforming slightly their density as the bigger atomic quadrupole moments evidence. The nitrogen atom, on its own, contracts itself into a rather oblate density distribution. The contraction is that of the density as a whole; however, there is an elongation of the valence shell charge concentration along the internuclear axis. The decrease in bond distances affects just quantitatively the values of densities and Laplacians at bond points, both following the exponential laws mentioned above.

C. Chemical Bond in MN₂ and M₂N₂ Isomers. The introduction of a second nitrogen atom changes the scenario completely, and the basic bonding features in these clusters come from the appearance of a clearly shaped nitrogen molecule weakly bonded to metal atoms or dimetal molecules. Topologi-

TABLE 5: Density (ρ) and Laplacian of the density ($\nabla^2\rho$) at Bond Critical Points for Clusters Containing Dinitrogen Molecules^a

	bond	<i>r</i>	ρ	$\nabla^2\rho$	bond	ρ	$\nabla^2\rho$
AlN ₂	Al–N	0.58	0.038	0.140	N–N	0.575	–1.592
GaN ₂	Ga–N	0.51	0.028	0.093	N–N	0.603	–1.765
InN ₂	In–N	0.48	0.017	0.056	N–N	0.614	–1.848
Al ₂ N ₂ <i>D</i> _{2h}	Al–N	0.59	0.046	0.179	N–N	0.422	–0.792
Ga ₂ N ₂ <i>D</i> _{2h}	Ga–N	0.52	0.054	0.173	N–N	0.446	–0.910
In ₂ N ₂ <i>D</i> _{2h}	In–N	0.49	0.043	0.142	N–N	0.467	–1.012
Al ₂ N ₂ <i>C</i> _{∞v}	Al–N	0.58	0.049	0.271	N–N	0.571	–1.563
					Al–Al	0.037	–0.024
Ga ₂ N ₂ <i>C</i> _{∞v}	Ga–N	0.44	0.001	0.003	N–N	0.637	–2.018
					Ga–Ga	0.036	0.008
In ₂ N ₂ <i>C</i> _{∞v}	In–N	0.63	0.001	0.003	N–N	0.637	–2.014
					In–In	0.026	0.021

^aAn asymmetry index $r = d_N/d$, where d_N is the distance from the bond point to the nitrogen atom and d is the total bond distance, is also shown for the metal–nitrogen bonds. All data in atomic units.

TABLE 6: Atomic Properties for Clusters Containing N₂ Molecules

	atom	proximal			distal		
		\mathcal{O}	μ	Q_b	\mathcal{O}	μ	Q_b
AlN ₂	Al	0.429	1.305	4.402	0.017	0.665	1.482
	N	–0.446	0.889	1.770			
GaN ₂	Ga	0.205	0.544	5.272	0.009	0.636	1.432
	N	–0.214	0.689	1.963			
InN ₂	In	0.144	0.420	6.542	0.011	0.619	1.385
	N	–0.151	0.674	1.734			
Al ₂ N ₂ <i>D</i> _{2h}	Al	0.794	–1.837	1.001			
	N	–0.794	0.742	3.106			
Ga ₂ N ₂ <i>D</i> _{2h}	Ga	0.526	1.223	2.155			
	N	–0.526	0.748	1.912			
In ₂ N ₂ <i>D</i> _{2h}	In	0.477	1.195	3.154			
	N	–0.476	0.785	1.778			
Al ₂ N ₂ <i>C</i> _{∞v}	Al	0.194	–1.766	7.601	0.297	0.824	2.580
	N	–0.535	0.964	1.964			
Ga ₂ N ₂ <i>C</i> _{∞v}	Ga	0.014	0.244	0.937	–0.008	0.315	0.218
	N	–0.005	0.614	1.270			
In ₂ N ₂ <i>C</i> _{∞v}	In	0.013	0.205	0.731	–0.005	0.276	–0.069
	N	–0.008	0.613	1.284			

^a The table contains the atomic charge, atomic dipole moment, and atomic quadrupole moment eigenvalue along (or nearest) the bond direction for all the atoms involved. All magnitudes in atomic units and all the symbols and conventions as in Table 2, except that when there is more than one bond, the dipole moment is taken as positive when it points toward the homonuclear bond direction.

cal and atomic properties, and Laplacian maps are found in Tables 5 and 6, and Figure 3, respectively.

In the case of the MN₂ systems, which are slightly deviated from linear configurations, charge transfers are much smaller than in the corresponding MN monomers and decrease from Al to In. The MN distances are also around 20% larger. Densities and Laplacians at the bond critical points have decreased according to this change in bond distance. For AlN₂, the shape of the metal valence shell and its atomic dipole moment are rather similar to those found in AlN, but the slight bending of the molecule alters the atomic quadrupole moments significantly. The curvature of the Al–N interatomic surfaces is still convex, but to a lesser extent. Interestingly, the unpaired electron spin density is rather equally shared by the Al (0.522 electrons) and the two nitrogens of the N₂ molecule (0.187 proximal, 0.291 distal). With regard to Ga and In molecules, both the charge transfer from the metal and the atomic dipole moments are about a third of those found in the corresponding diatomics, and not much relevant structure is present except a small electron polarization against the N₂ molecule. As far as

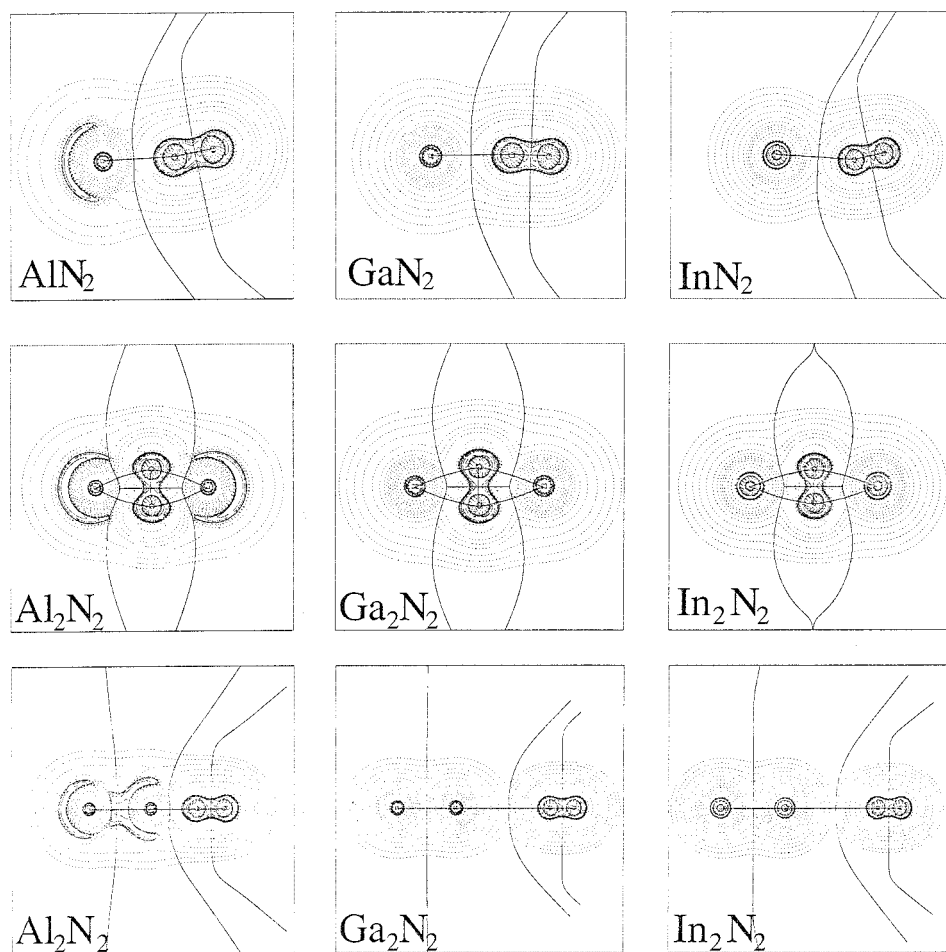


Figure 3. Laplacians of the electron density for clusters containing dinitrogen molecules in a plane containing all nuclei. The geometries are those predicted at equilibrium.

the latter is concerned, all the transferred charge is actually accumulated in the proximal nitrogens, which become in return very slightly more forward polarized than in the isolated dinitrogen molecule. On the other hand, we may say confidently that the distal nitrogens are mostly unaltered. A very interesting feature is the charge dependent elongation of the N–N distance, on which further comment will be made below. As we move from Al to In, the spin density tends to get localized in the metal atoms: 0.737 extra α electrons in Ga and 0.831 in In, with an almost equal share of the rest among the nitrogens in both.

Comparing them with the MN_2 clusters, the D_{2h} rhombic configurations of the M_2N_2 clusters display the same type of charge transfer enhancement found on going from the MN to the M_2N molecules, though now the change in the AlN distance (around 3%) is much smaller than in the GaN or InN cases (around 12%). The charge transfers approach the values in the MN diatomics, suggesting a relation with the MN distance that will be further investigated below. Moreover, the M atomic dipoles are very similar to those in the MN or M_2N molecules. On the other hand, the N–N bond has weakened substantially, suggesting also a very interesting relation among the number of metal atoms present, their distance to the N_2 molecule and the strength of the N–N bond.

We finally consider the linear M_2N_2 isomers. The aluminum cluster has interesting features, consisting of an Al_2 molecule with a slightly expanded bond distance with respect to the isolated one, carrying a positive net charge of 0.491 electrons (0.194 proximal, 0.297 distal), and a N_2 molecule with a proximal nitrogen bearing almost that negative charge. The distal

nitrogen, as in previous examples, is slightly positive. The Al–N distance is appreciably smaller than that in the AlN_2 cluster. Both aluminums are clearly back-polarized. The proximal is very similar (comparing the atomic dipoles) to all the other Al atoms we have encountered, and the distal behaves as a very slightly distorted Al in Al_2 . Notice that the proximity of the nitrogen molecule is able to reverse the sign of the atomic dipole in the distal Al atom. This severe polarization does not modify appreciably the Al–Al bond if, of course, the bond distance difference is accounted for. The nitrogen molecule, on the other hand, displays exactly the same pattern already examined.

Ga_2N_2 and In_2N_2 have very large metal nitrogen distances, falling in the dominion of van der Waals interactions. DFT, even gradient corrected versions of it, must be used carefully in these cases,^{13,14} particularly when energetic properties are considered. However, density features are more reliable. A measure of that reliability is the comparison of the optimized geometries in the dinitrogen and dimetal molecules with the linear dimer. Table 1 shows that our optimized clusters display interatomic distances almost identical to those in the isolated diatomics. Moreover, in both cases the charge transfers are negligible, so the N_2 and dimetal molecules are mostly neutral slightly forward and backward polarized species, respectively. In neither case the proximal metal atom is perturbed enough to reverse the sign of its atomic dipole moment.

IV. Discussion and Conclusions

Besides the specific characterization of the bonding properties of each of the clusters here studied, there are several interesting

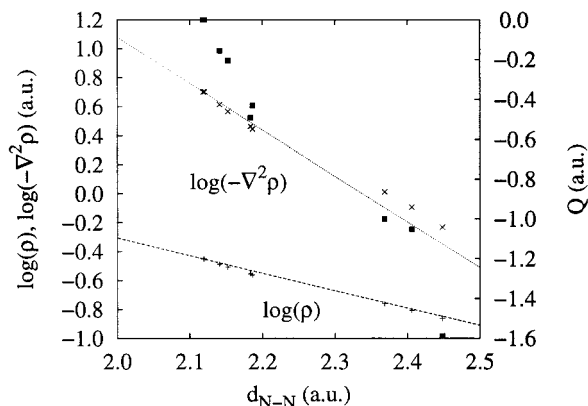


Figure 4. Density (+) and Laplacian of the density (\times) versus N–N internuclear distance at the N–N bond critical point in the MN_2 , M_2N_2 , and M_2N_2 clusters. Each symbol corresponds to one of the clusters studied. Lines stand for the values computed in the isolated neutral N_2 molecule at several internuclear distances. Filled squares (right y axis labeled) stand for the total charge transferred from the metal atoms to the N_2 molecule.

features emerging from the overall analysis of the results. The one of most importance is the relevance of electrostatic interactions in the understanding of these compounds. Except Al clusters, for which complex deformations of the Al valence shell and noticeable reorganization of the electron densities are found, all Ga and In molecules display nonshared polar interactions.

Another interesting point of general applicability is the simple exponential relation between densities and Laplacians at the bond critical points and bonding distance for a given pair of atoms. This behavior has also been found valid for other kinds of interactions and a wide range of distances. These cover the bonding regimes going from short distances, shared interactions through long-range, van der Waals ones.^{11,12} Figure 4 shows this exponential relation for the N–N bond critical point in all our clusters displaying it. The solid lines are the values obtained for the neutral N_2 molecule at a grid of internuclear distances. The somewhat greater values of the Laplacian found for N–N distances around 2.4 bohr correspond to the rhombic clusters. Those values are explained easily if we take into account the softening of the perpendicular negative curvatures of the N–N density at the critical point due to the metals in front. In fact, if we plot the value of the curvature of the density along the interatomic line instead of the Laplacian, the agreement of these points is as good as that found in the density plot. Similar images are obtained for the MN and MM bond critical points. A particularly interesting fact here is that there is a clear correlation between the total charge transferred to the N_2 molecule and its internuclear distance. The answer to the question of how can the density and the Laplacian at the N–N critical point follow so closely the values found for the neutral diatomic with such big charge transfers may lie in the strong localization of that transferred charge in the proximal nitrogen. Moreover, this transferred charge is polarized toward the metal atoms, in the opposite direction to the N–N internuclear axis. The region near the N–N bond is not affected much by the process. The accumulation of charge tends to minimize as much as possible the effect over the strong dinitrogen bond.

An equivalent situation is found in the dimetal molecules of the linear M_2N_2 clusters. In the aluminum system a rather large charge is transferred from the Al_2 molecule to the N_2 one. As a result, both the Al–Al and N–N distances increase noticeably, and densities at their associated bond point decrease following exponential laws. The negligible charge transfers found in the

In and Ga cases imply almost unaltered isolated dimetal and dinitrogen molecules.

These facts are in agreement with previous findings, pointing toward the existence of a universal set of bonding regimes for a given pair of atoms, mainly related to bond distance.^{10,11} In each particular case, the factors determining which specific equilibrium distances are chosen may change. Here we have shown how the transfer of nonnegligible amounts of charge is the driving force behind the distance change and how the redistribution of charge following the transfer achieves a minimum change in the density along the internuclear axes. Bond length is seen to determine the dominant type of interaction between atoms and also the final density found at the bond critical point.

The clusters studied in this work are remarkable in many aspects. By changing the metal atom and/or the relative stoichiometry of nitrogen atoms in the clusters, we include most of the known bonding regimes. When moving from Al to In, we observe a trend toward nonshared interactions and a softening of the curvatures of the electron density in the bonding regions. Valence electrons become more labile or metallic. In this process, charge transfers decrease and spin localization increases. Only the aluminum molecules show visible distortions in their valence shells and should be considered more or less covalent. Moreover, the presence of two nitrogen atoms leads to the formation of a dinitrogen molecule in all the clusters studied here. Nitrogen atoms are efficient sinks of charge, and the final charge transfers control the electrostatic interactions with the metal atoms.

We have found in this work that the atoms in molecules theory gives a detailed and consistent picture of the chemical bond in the nitride polyatomics. All that is needed is a reliable electron density, and much more could be said if the same type of reliability could be achieved for the nondiagonal first-order and second-order density matrices. A number of “classical” bonding types are present in these systems, and they are all treated on the same footing. As a result of this balance, electrostatic forces from polarized densities are found to be very important for the stability of the clusters. Even in the aluminum molecules, with sometimes large charge transfers and deformed valence shells, this model is still basically valid. The presence of two nitrogen atoms introduces a very strong covalent bond between them. That bond is a function of the charge transfer, and its properties closely follow those in the isolated molecule. We may infer that given a sufficient number of metal atoms surrounding an N_2 molecule, its large stability will have to compete with that of conformations without the N–N bond but with an increasing number of M–N weaker bonds. This is an interesting direction for continuing our efforts.

Acknowledgment. A.M.P. and M.A.B. are indebted to the Spanish Secretaría de Estado de Universidades, Investigación y Desarrollo, for support in their foreign stays. A.M.P., A.C., J.M.R., and M.A.B. are also indebted to the Spanish DGICYT for Grant PB96-0559.

References and Notes

- (1) Kandalam, A.; Pandey, R.; Blanco, M. A.; Costales, A.; Recio, J. M.; Newsam, J. M. *J. Phys. Chem. B*, previous paper in this issue.
- (2) Belyanin, A. F.; Bouilov, L. L.; Zhirnov, V. V.; Kamenev, A. I.; Kovalskij, K. A.; Spitsyn, B. V. *Diam. Relat. Mater.* **1999**, *8*, 369.
- (3) Bader, R. F. W. *Atoms in Molecules*; Oxford University Press: Oxford, U.K., 1990.
- (4) *Dmol user guide*, version 2.3.6; Molecular Simulations, Inc.: San Diego, CA, 1995.

- (5) Keith, T. A.; Laidig, K. E.; Krug, P.; Cheeseman, J. R.; Bone, R. G. A.; Biegler-König, F. W.; Duke, J. A.; Tang, T.; Bader, R. F. W. *The aimpac95 programs*; 1995.
- (6) *Gaussian 98*; Gaussian, Inc.: Pittsburgh, PA, 1998.
- (7) Becke, A. D. *Phys. Rev. A* **1988**, 38, 3098.
- (8) Perdew, J. P.; Wang, Y. *Phys. Rev. B* **1992**, 45, 13244.
- (9) *Extensible computational chemistry environment basis set database*, version 1.0; Molecular Science Computing Facility, E.; Laboratory, M. S.; Pacific Northwest Laboratory: Richland, WA, 1999.
- (10) Martín Pendás, A.; Blanco, M. A.; Costales, A.; Mori-Sánchez, P.; Luaña, V. *Phys. Rev. Lett.* **1999**, 83 (10), 1930.
- (11) Luaña, V.; Costales, A.; Mori-Sánchez, P.; Martín Pendás, A., unpublished.
- (12) Martín Pendás, A.; Costales, A.; Luaña, V. *J. Phys. Chem.* **1998**, 102, 6937.
- (13) Patton, D. C.; Pederson, M. R. *Int. J. Quantum. Chem.* **1998**, 69, 610.
- (14) Dobson, J. F. *Int. J. Quantum. Chem.* **1998**, 69, 615.